

Effect of plasticity on elastic modulus measurements

Donald J. Weidner, Li Li, Maria Davis, and Jihua Chen

Department of Geosciences, State University of New York at Stony Brook, Stony Brook, New York, USA

Received 17 November 2003; accepted 9 February 2004; published 27 March 2004.

[1] Recent developments in high-pressure X-ray studies enable the measurement of the elastic strain anisotropy induced by a macroscopic differential stress in an aggregate sample. Such data are commonly used to constrain the single-crystal elastic moduli under the assumptions of the Reuss-Voigt state. We find this procedure is valid only for samples that have not been plastically deformed. Measured elastic strain anisotropy for MgO at stress levels below the yield point agree well with the Reuss elastic model. Plastic deformation effects a change in the stress field for subpopulations of grains that represent different crystallographic orientations with respect to the applied stress field. Our data for the plastically deformed sample are consistent with the predictions of a self-consistent aggregate model for deforming polycrystals. Such models may be useful as a guide to define the elastic properties in light of the active slip systems. *INDEX TERMS:* 3902 Mineral Physics: Creep and deformation; 3909 Mineral Physics: Elasticity and anelasticity; 3924 Mineral Physics: High-pressure behavior; 3954 Mineral Physics: X ray, neutron, and electron spectroscopy and diffraction; 3994 Mineral Physics: Instruments and techniques. *Citation:* Weidner, D. J., L. Li, M. Davis, and J. Chen (2004), Effect of plasticity on elastic modulus measurements, *Geophys. Res. Lett.*, *31*, L06621, doi:10.1029/2003GL019090.

1. Introduction

[2] Seismic models of the deep Earth continue to provide a rich view of the materials and processes that shape the planet. Anisotropy has been proved to be a key characteristic that enlightens us about the nature of plate motions [Silver and Holt, 2002], the structure of the core-mantle boundary [Garnero and Lay, 1997], and the rotation of the Earth's inner core [Tromp, 2001]. To interpret these geophysical observations, we require knowledge of single crystal elastic moduli of minerals at deep Earth conditions, as it is the anisotropy that distinguishes single-crystal elasticity from the elastic bulk and shear moduli. The development of synchrotron based piezometers [Singh, 1993] has given impetus to new techniques that enable the determination of elastic anisotropy [Singh et al., 1998].

[3] X-ray transparent gaskets and anvils allow measurement of elastic strain for oriented subsets of grains within a polycrystalline sample under uniaxial stress at high pressure. If elastic anisotropy controls the stress-strain state, then the measured elastic strain anisotropy reflects the elastic modulus anisotropy. This has been used to characterize the single-crystal elastic properties of iron [Mao et al.,

1998], MgO [Merkel et al., 2002], ringwoodite [Kavner, 2003; Kavner and Duffy, 2001], and stishovite [Shieh et al., 2002]. However, several recent studies of deforming materials [Daymond and Bonner, 2003], using neutron scattering to define elastic strain, demonstrate that the elastic strain is controlled by the plastic anisotropy once plastic flow is initiated.

[4] In this paper, we investigate the effect of plastic flow on the stress state of a polycrystalline sample. Data taken for MgO, at a stress state both above and below the yield point are examined. Plastic flow considerably changes the stress distribution among the subpopulations of grains. These observations are consistent with a Reuss model only in the elastic regime but with the predictions from a self-consistent model for deformation of a polycrystal based on dislocation creep in the plastic region. In fact, many of the reported results using elastic strain anisotropy to determine elastic moduli are flawed because the plastic anisotropy controls the observations.

2. Elastic Moduli From X-Ray Diffraction

[5] We examine the manner that elastic properties are deduced from static measurements of X-ray diffraction for a cubic-symmetry material under uniaxial stress. The conclusions drawn in this case are also applicable to all crystal symmetries. A subpopulation of grains that are identified by their diffraction vector, hkl , that are all under the same uniaxial stress field, can be characterized by a strain metric by $\epsilon^{hkl} = (\epsilon_1 - \epsilon_3)^{hkl}$. The strains, ϵ_1 and ϵ_3 , are measured parallel and perpendicular to the maximum compressive direction [Singh, 1993]. ϵ^{hkl} represents the differential strain for the grain subpopulation corresponding to the particular diffraction peak, (hkl). From this we can define the differential stress of grain subpopulations as in equation (1):

$$\sigma^{hkl} = (\sigma_1 - \sigma_3)^{hkl} = E^{hkl} \epsilon^{hkl} \quad (1)$$

where E^{hkl} is the Young's modulus corresponding to the (hkl) direction in the crystal. In the case of cubic symmetry, this becomes as equation (2) [Singh, 1993]:

$$\begin{aligned} \sigma^{hkl} &= (S_{11} - S_{12})^{-1} \epsilon^{hkl} \quad \text{for } hkl = 200 \\ \sigma^{hkl} &= (S_{44}/2)^{-1} \epsilon^{hkl} \quad \text{for } hkl = 111 \\ \sigma^{hkl} &= [1/4(S_{11} - S_{12}) + 3S_{44}/8]^{-1} \epsilon^{hkl} \quad \text{for } hkl = 220 \end{aligned} \quad (2)$$

The stress field for other diffraction peaks are related to the strain by a linear combination of the elastic compliance moduli, S_{44} and $(S_{11} - S_{12})$ [Singh, 1993].

[6] The recent breakthroughs using X-ray transparent anvils or gaskets [Li et al., X-ray strain analysis at high

pressure: The Effect of plastic deformation in MgO, submitted to Phys. Earth Planet. Inter.; *Mao et al.*, 1998] allow the measurement of ε^{hkl} for several diffraction peaks. If the elastic properties are well known, then equation (2) will yield the stress for the different subpopulations of grains that define the diffraction peak. Information about the elastic properties may also be obtained if more information about the stress-strain field is known. In the cubic crystal case, we wish to examine the elastic strain anisotropy, ξ , represented by the ratio of the elastic strains of the (200) and the (111) diffraction peaks:

$$\begin{aligned}\xi &= \varepsilon^{200}/\varepsilon^{111} \\ &= 2(S_{11} - S_{12})/S_{44}(\sigma^{200}/\sigma^{111}) \\ &= A(\sigma^{200}/\sigma^{111})\end{aligned}\quad (3)$$

where A is the elastic modulus anisotropy of the material. With additional constraints, such as the Reuss-Voigt bounds [Reuss, 1929; Voigt, 1928], this equation defines limits on the elastic modulus anisotropy, A , given the measurement of the elastic strain anisotropy, ξ . The most often used bound, the Reuss bound, assumes uniform stress on all parts of the sample, requiring that the stress on each subpopulation be equal. Thus, the elastic strain anisotropy, ξ , will be a proxy for the elastic modulus anisotropy, A . If the actual elastic state is closer to the Voigt bound, then the subpopulation experiencing the largest strain will correspond to the grains bearing the smallest stress as the material state is represented by a compromise between uniform stress and uniform strain. As a result, by equation (3), the strain anisotropy, ξ , will be closer to one than it is to the elastic modulus anisotropy, A .

[7] In order to gain information on the actual values of the elastic moduli, rather than just the elastic modulus anisotropy, A , both the average differential stress, $\langle\sigma^{hkl}\rangle$, and the pressure need to be defined [Singh et al., 1998]. Thus, to determine the three elastic moduli of a cubic material, the most common procedure includes the following:

[8] 1. Input the bulk modulus, K_T , from other studies.

[9] 2. Input or estimate the shear modulus, μ , from other studies.

[10] 3. Infer the elastic modulus anisotropy from the elastic strain anisotropy. The values of the bulk and shear moduli may come from other experiments, such as Brillouin spectroscopy, or from ultrasonic velocity measurements on polycrystalline samples. Furthermore, as we discuss below, the elastic strain anisotropy may not reflect the elastic modulus anisotropy if plastic flow has been operative in the sample.

3. Effect of Plasticity

[11] Several recent studies report that the elastic strain anisotropy, ξ , in equation (3) changes dramatically as a material is stressed from the elastic region to the plastic region [Clausen, 1997; Daymond and Bonner, 2003; Li et al., 2004]. It is suggested [Clausen, 1997] that the controlling features of the stress-strain field in the plastic region are the orientations and strength of the dislocation slip planes.

Furthermore, the elastic strain no longer represents the total strain of the individual grains as plastic strain quickly becomes dominant. The X-rays can only detect elastic strain.

[12] Bounding states similar to the Reuss-Voigt limits have been defined by Taylor [Taylor, 1938] (uniform strain) and Sachs [Sachs, 1928] (uniform stress) for plastically deforming materials. The Taylor model [Taylor, 1938] for calculating the uniaxial stress-strain relation for an aggregate requires five independent slip systems to accommodate the five independent strain components for plastic deformation [von Mises, 1928]. The plastic strain is homogeneous and independent of grain orientation in the Taylor model. Stresses are related to the geometry of the grains relative to the stress field and the slip systems. The Sachs model [Sachs, 1928], which is also called the extreme lower-bound, regards the aggregate as having the same stress for all grains. Again, the stress-strain field is governed by the geometry and strength of the active dislocation orientations.

[13] A self-consistent model [Hutchinson, 1970] is placed in between the upper-bound Taylor model and the lower-bound Sachs model. This model is governed by the single crystal slip mechanisms. Both the elastic anisotropy, A , and the plastic anisotropy, (the different critical resolved stress on each slip system and the hardening laws [Clausen, 1997]) are incorporated into the self-consistent models. This model predicts strain and stress for different subpopulations of grains which is comparable to the measured stress and strain for related (hkl) diffractions.

4. Observations

[14] Two separate experiments were conducted with the DDIA high-pressure deformation device [Wang et al., 2003]. In the experimental run MgO42, a polycrystalline MgO sample was placed in series with two single crystals along the deformation axis. As the anvils are driven into the sample chamber, both single crystals exhibited considerable shortening while the polycrystalline sample produced no measurable plastic deformation. In run Tan02, a similar cell design is used but the MgO polycrystalline sample was in series with a tantalum rod and experienced higher stress with the result that there was significant plastic deformation. The data presented here are all for 500°C. In run MgO42, the pressure was 5.7 (± 0.5) GPa and run Tan02 operated at two pressures: 2.3 and 4.5 (± 0.5) GPa. Further details of the cell assembly and experimental protocols are reported elsewhere [Li et al., 2004].

[15] Figure 1 illustrates the measured elastic strain anisotropy, ξ . Also plotted in this figure are solid lines corresponding to the elastic modulus anisotropy predicted from acoustic single crystal measurements [Sinogeikin and Bass, 1999; Spetzler, 1970], which should represent the elastic strain anisotropy if the Reuss state is realized. Dashed lines are the predictions of this quantity using a self-consistent plasticity model [Clausen, 1997; Hutchinson, 1970]. The sample with no plastic deformation (in run MgO42) displays an elastic strain anisotropy that is consistent with the elastic modulus anisotropy. The samples which were plastically deformed exhibit an elastic strain anisotropy that is consistent with the plasticity models.

[16] The elastic strain anisotropy was calculated for a plastically deforming solid using the program of [Clausen,

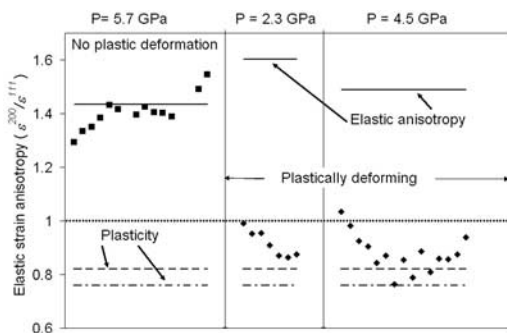


Figure 1. The elastic strain anisotropy of MgO from D-DIA experiments at a temperature of 770 K. The left set of data (square symbols) are from Run MgO42 which has no plastic deformation and carried out at 5.7 GPa. The center and right set of data (diamond symbols) are from Run Tan02 which is under plastic deformation at 2.3 GPa and 4.5 GPa respectively. The experimental data points are individual diffraction spectra collected sequentially at time intervals of approximately 10 minutes with a constant applied stress field. The solid lines correspond to the elastic modulus anisotropy predicted from acoustic single crystal measurements [Sinogeikin and Bass, 1999; Spetzler, 1970]. The dash-dot lines are the predictions of this quantity using a self-consistent plasticity model [Clausen, 1997; Hutchinson, 1970] with slip planes of $\{111\}$, $\{110\}$, and $\{100\}$ activated, and slip in the $\langle 110 \rangle$ direction. The dashed line is for slip on $\{111\}$ planes only.

1997]. The results depend on the activated slip systems. When slip planes of $\{111\}$, $\{110\}$, and $\{100\}$ are all activated, with slip in the $\langle 110 \rangle$ direction, the calculated the elastic strain anisotropy is 0.76. When only the $\{111\}$ slip system is active, then the elastic strain anisotropy is 0.82. If plasticity relies mostly on the $\{110\}$ slip system, the elastic strain anisotropy is 0.23. We see that the model with active slip on the $\{111\}$ plane fits our data the best, but the model with active slips on all three systems fits fairly well. Actual slip mechanisms of MgO at high pressure are still poorly identified. At room temperature, the $\{110\}$ $\langle 110 \rangle$ slip systems are reported to dominate [Merkel *et al.*, 2002], while at higher temperature slip on $\{111\}$ and $\{100\}$ may become active [Wenk, 2002].

[17] We conclude that the Reuss-Voigt model is valid for the sample that is not plastically deforming and the Reuss bound appears to explain the data from elastically deformed sample very well. When we use this data from the non-plastically deformed MgO experiment to define the elastic moduli of MgO, the result is consistent with acoustic data. However, once plasticity is active, the Reuss-Voigt bounds no longer apply and the strain anisotropy changes from greater than one to less than one (which is commonly referred as the change of the sign for anisotropy) as the (111) peak shows the greater elastic strain. This agrees with the prediction from the self-consistent model that the stresses in the different subpopulations of grains become quite different after the onset of plastic deformation, with the stress on the (111) subpopulation of grains becoming over 50% greater than for the (200) subpopulation of grains. The prediction from the self-consistent model agrees quite well with the observed elastic strain after plastic deforma-

tion occurs. If we would use the elastic strain anisotropy of the plastically deforming sample to predict the elastic modulus anisotropy, A , we would not even get the correct sign for the departure from isotropy.

[18] A recent diamond anvil study of MgO [Merkel *et al.*, 2002] reported strength and elastic properties of MgO from such measurements. The measured elastic strain anisotropy is illustrated in Figure 2 as a function of pressure for the low pressure portion of their data. Their very lowest pressure data yield results that agree with A , but ξ decreases very rapidly and becomes compatible with the plasticity model by 5 GPa. We suggest that their sample behaved elastically until the differential stress was large enough to plastically deform the MgO. When this happened, the elastic strain anisotropy, ξ , decreased rapidly as the stress distribution between subpopulations redistributed. Beyond this point, the elastic strain anisotropy, ξ , is probably governed by the plastic properties and only indirectly by the elastic moduli.

[19] Kavner and others [Kavner, 2003; Kavner and Duffy, 2001] report the strength and elastic properties of ringwoodite and hydrous ringwoodite. They note that the elastic strain anisotropy, ξ , in their studies are significantly different from the elastic modulus anisotropy, A , from Brillouin data [Sinogeikin *et al.*, 2003]. The results are illustrated in Figure 3. Also indicated here are the elastic strain anisotropy, ξ , calculated using the MgO self-consistent model.

[20] The diamond-anvil-cell X-ray data agree quite well with the prediction from the self-consistent model and are discrepant with the elastic modulus anisotropy, A . Again, the stress of the diamond-anvil-cell probably induces plastic flow, and the plastic properties dominate the elastic strain-stress state of the material.

5. Discussion

[21] Plastic creep by way of dislocation movement is controlled by the crystallographic orientations of the dislocations. This imposes a strong anisotropy on the stress-strain field that is required to activate slip on these

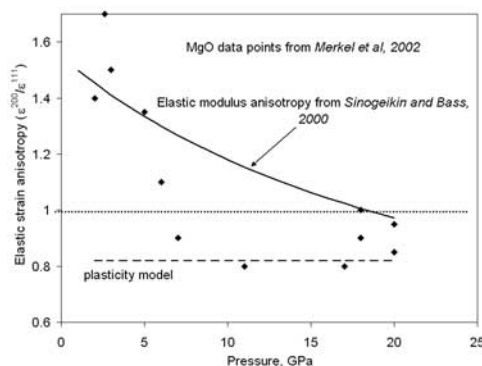


Figure 2. Elastic strain anisotropy for MgO as a function of pressure at room temperature. The data of Merkel *et al.* [2002] for pressure less than 20 GPa are illustrated. The elastic modulus anisotropy from Sinogeikin and Bass [1999] (solid line) illustrates the elastic strain anisotropy that is predicted by the Reuss state. The predicted elastic strain anisotropy (dashed line) is from the self-consistent plasticity model with active dislocation systems on $\{111\}$ planes in the $\langle 110 \rangle$ direction.

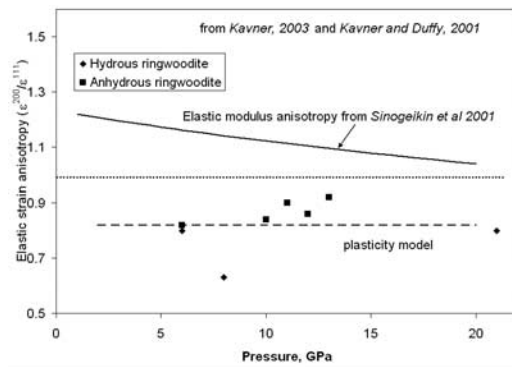


Figure 3. Elastic strain anisotropy for ringwoodite (square symbols) and hydrous ringwoodite (diamond symbols) as a function of pressure at room temperature [Kavner, 2003; Kavner and Duffy, 2001]. The elastic modulus anisotropy from Sinogeikin et al. [2003] (solid line) illustrates the elastic strain anisotropy that is predicted by the Reuss state. The predicted elastic strain anisotropy (dashed line) is from the self-consistent plasticity model for MgO with active dislocation systems on $\{111\}$ planes in the $\langle 110 \rangle$ direction.

dislocations. Systems as multiply distributed as the $\{111\}$ slip plane with $\langle 110 \rangle$ slip, with 12 equivalent systems in the cubic symmetry, still produces stresses within the grains that vary by 50% between subpopulations. In fact, it is these subpopulations that are sampled with X-ray diffraction. As a result, the elastic strain anisotropy, ξ , in equation (3) cannot be used to estimate the elastic modulus anisotropy, A , since the stress is not uniform in different subpopulations of grains.

[22] The advanced development in high pressure diffraction experiments has rendered sufficient precision to measure elastic strains that are caused by stresses that are less than the yield point as well as the orientation control allowing access to several directions within the specimen thus examination of the differential strain field. We can capitalize on these new capabilities to gain insights into both the elastic and plastic processes that are controlling the stress-strain relationship. We suggest that the static X-ray diffraction method for determining elastic properties should be restricted to stress fields that are lower than the yield strength of the material. One possible solution to avoid the effect of plasticity in the elasticity measurement is to remove the stress and strain by annealing the sample once the sample is at the target pressure, and then further compress to impose a fresh differential stress field onto the sample that is within the sample elastic limit. Elastic modulus anisotropy, A , can be measured, but as we see here, these measurements are seriously deteriorated by plastic deformation.

[23] **Acknowledgments.** Funding was provided by the National Science Foundation grants: EAR0135551 and EAR0229260, an REU program

EAR 0139436 and by the support to NLSL Beamline X17B2 through COMPRES (EAR 0135554) at Brookhaven National Laboratory. This is MPI publication 342. We thank Dr. W. B. Durham, Dr. P. Burnley, and Dr. B. Clausen, for equipment, inspiration, and software.

References

- Clausen, B. (1997), Characterization of polycrystal deformation by numerical modelling and neutron diffraction measurements, Ph.D. thesis, Riso Natl. Lab., Roskilde, Denmark.
- Daymond, M. R., and N. W. Bonner (2003), Lattice strain evolution in IM1834 under applied stress, *Mater. Sci. Eng. A*, *340*, 272–280.
- Garnero, E. J., and T. Lay (1997), Lateral variations in lowermost mantle shear wave anisotropy beneath the North Pacific and Alaska, *J. Geophys. Res.*, *102*, 8121–8135.
- Hutchinson, J. W. (1970), Elastic-plastic behavior of polycrystalline metals and composites, *Proc. R. Soc. London, Ser. A*, *319*, 247.
- Kavner, A. (2003), Elasticity and strength of hydrous ringwoodite at high pressure, *Earth Planet. Sci. Lett.*, *214*, 645–654.
- Kavner, A., and T. S. Duffy (2001), Strength and elasticity of ringwoodite at upper mantle pressures, *Geophys. Res. Lett.*, *28*, 2691–2694.
- Li, L., P. Raterron, D. J. Weidner, and J. Chen (2003), Olivine flow mechanisms at 8 GPa, *Phys. Earth Planet. Inter.*, *138*, 113–129.
- Li, L., et al. (2004), X-ray stress analysis in deforming materials, *J. Appl. Phys.*, in press.
- Mao, H.-K., et al. (1998), Elasticity and rheology of iron above 220 GPa and the nature of the Earth's inner core, *Nature*, *296*, 741–743.
- Merkel, S., et al. (2002), Deformation of polycrystalline MgO at pressures of the lower mantle, *J. Geophys. Res.*, *107*(B11), 2271, doi:10.1029/2001JB000920.
- Reuss, A. (1929), Berechnung der Flie(grenze von Mischkristallen auf Grund den Konstanten des Einkristalls, *Z. Angew. Math. Mech.*, *9*, 49.
- Sachs, G. (1928), Zur Ableitung einer Fließbedingung, *Z. Ver. Dtsch. Ing.*, *72*, 734–736.
- Shieh, S. R., et al. (2002), Strength and elasticity of SiO₂ across the stishovite-CaCl₂-type structural phase boundary, *Phys. Rev. Lett.*, *89*.
- Silver, P. G., and W. E. Holt (2002), The mantle flow field beneath western North America, *Science*, *295*, 1054–1057.
- Singh, A. K. (1993), The lattice strains in a specimen (cubic symmetry) compressed nonhydrostatically in an opposed anvil device, *J. Appl. Phys.*, *73*, 4278–4286.
- Singh, A. K., et al. (1998), Estimation of single-crystal elastic moduli from polycrystalline X-ray diffraction at high pressure: Application to FeO and iron, *Phys. Rev. Lett.*, *80*, 2157–2160.
- Sinogeikin, S. V., and J. D. Bass (1999), Single-crystal elasticity of MgO at high pressure, *Phys. Rev. B*, *59*, R14,141–R14,144.
- Sinogeikin, S. V., et al. (2003), Single-crystal elasticity of ringwoodite to high pressures and high temperatures: Implications for 520 km seismic discontinuity, *Phys. Earth Planet. Inter.*, *136*, 41–66.
- Spetzler, H. (1970), Equation of state of polycrystalline and single-crystal MgO to 8 kilobars and 800K, *J. Geophys. Res.*, *75*, 2073–2087.
- Taylor, G. I. (1938), Plastic strain in metals, *J. Inst. Met.*, *62*, 307–315.
- Tromp, J. (2001), Inner-core anisotropy and rotation, *Annu. Rev. Earth Planet. Sci.*, *29*, 47–69.
- Vaughan, M., et al. (2000), Use of X-ray imaging techniques at high-pressure and temperature for strain measurements, in *AIRAPT-17*, edited by M. H. Manghni, W. J. Nellis, and M. F. Nicol, pp. 1097–1098, Univ. Press, Hyderabad, India.
- Voigt, W. (1928), *Lehrbuch der Kristallphysik*, Teubner, Berlin.
- von Mises, R. (1928), *Mechanik der Plastischen Formänderung von Kristallen*, pp. 161–185.
- Wang, Y. B., et al. (2003), The deformation-DIA: A new apparatus for high temperature triaxial deformation to pressures up to 15 GPa, *Rev. Sci. Instrum.*, *74*, 3002–3011.
- Wenk, R. (2002), Texture and anisotropy, in *Plastic Deformation of Minerals and Rocks*, edited by S. Karato and R. Wenk, pp. 291–329, Mineral. Soc. of Am., Washington, D. C.

J. Chen, M. Davis, L. Li, and D. J. Weidner, Department of Geosciences, State University of New York at Stony Brook, Stony Brook, NY 11794, USA. (dweidner@sunysb.edu)